

# LPB as a Crack Initiation Resistant Process for Case Hardened Steels

N. Jayaraman, Doug Christensen, Jeremy Scheel  
Lambda Research  
5521 Fair Lane  
Cincinnati, Ohio 45227-3401

## Abstract

The high cycle fatigue performance of case carburized 9310 rotorcraft gear steel was investigated with shot peening (SP), low plasticity burnishing (LPB), and as-ground surface conditions to compare the relative resistance to crack initiation. A 0.010 in. (0.25 mm) EDM notch was used to simulate damage frequently encountered in rotorcraft gears such as contact fretting induced pitting. In the smooth (undamaged) condition LPB leads to a 10% improvement in fatigue strength over SP and a 20% improvement over the as-ground condition, and in the presence of simulated damage, to a 100% improvement over SP. Residual stress relaxation due to both mechanical and thermal exposure was also investigated. Both LPB and SP lead to similar residual stress relaxation on the surface after a single cycle of mechanical overload. Below the surface, SP leads to either a complete relaxation of the residual compression or a transition into residual tension after the overload cycle, while LPB leads to stable compressive residual stresses. This study paves the way for developing applications of LPB technology for rotorcraft gear components by appropriate design of LPB tools and implementation of the designed residual stresses to improve the fatigue performance and damage tolerance.

## INTRODUCTION

The high cycle fatigue (HCF) performance of rotorcraft drive train components, such as gears, shafts, and bearings, has long been improved by the introduction of a shallow surface layer of compressive residual stress by shot peening<sup>1,2,3</sup>. These components are typically manufactured from high strength case carburized steels such as 9310 steel. To achieve the desired dimensional precision, the parts are typically finish ground and SP as a final step to enhance the fatigue strength. Achieving greater depth and magnitude of compression through heavier or higher intensity peening may further improve the fatigue performance, yet will produce unacceptable levels of cold work and surface roughness. It has been shown that the rough surface finish introduced by peening processes can lead to a serious debit in the fatigue performance of high strength case carburized steels.<sup>4,5,6</sup> High levels cold work or plastic deformation associated with the SP processes lead to relaxation of the beneficial compressive residual stresses when the parts are exposed to moderately elevated temperatures and mechanical overload conditions.<sup>7,8,9</sup> LPB processing offers the combined advantages of controlled depth and magnitude of residual compression, mirror-like smooth finish, and controlled, very low cold work. LPB costs are comparable to conventional SP processes, generating a highly favorable cost-benefit ratio.

## EXPERIMENTAL PROCEDURE

### Material

9310 steel was acquired in the AMS 6265M condition. A total of 62 HCF specimens with finished dimensions of 0.375 x 1.25 x 8 in. (9.5 x 31.75 x 203.2 mm) and 10 thermal relaxation and 3 point bend specimens with finished dimensions of 0.375 x 1.25 x 12 in. (9.5 x 31.75 x

304.8 mm) were machined from the bar stock. All specimens were carburized and heat treated per Rolls-Royce's process specification EPS200 to achieve a surface hardness of 62 Rc and a depth of carburized layer of  $\approx 0.05$  in. (1.27 mm). Test specimens were subsequently machined to final dimensions. At least 0.005 in. (0.13 mm) of material was ground from each gage section to remove the decarburized layer before final processing.

### **Specimen Processing**

LPB process parameters were developed for both specimen types to achieve nominally 0.030 in. (0.76 mm) of compression. Samples were processed on a CNC mill to allow positioning of the LPB tool in a series of passes along the active gage region. LPB test specimens had an additional 0.005 in. (0.13 mm) of material removed by grinding after the LPB processing to correct specimen geometry after the quenching process. All SP was performed per Rolls Royce's process specification EPS12176G. Baseline specimens were left in the as ground condition after the decarburized layer was ground off.

### **Residual Stress and Retained Austenite Measurements**

X-ray diffraction residual stress measurements were performed using a  $\sin^2\psi$  technique employing the diffraction of Cr K-alpha 1 radiation from the (211) planes of the BCC structure of the 9310 gear steel. The diffraction peak angular positions at each of the psi tilts employed for measurement were determined from the position of the K-alpha 1 diffraction peak separated from the superimposed K-alpha doublet assuming a Pearson VII function diffraction peak profile in the high back-reflection region. The diffracted intensity, peak breadth, and position of the K-alpha 1 diffraction peak were determined by fitting the Pearson VII function peak profile by least squares regression after correction for the Lorentz polarization and absorption effects and for a linearly sloping background intensity.<sup>10,11,12,13</sup> Where appropriate, material was removed electrolytically for subsurface measurement in order to minimize possible alteration of the subsurface residual stress distribution as a result of material removal. The residual stress measurements were corrected for both the penetration of the radiation into the subsurface stress gradient<sup>14</sup> and for stress relaxation caused by layer removal.<sup>15</sup> The volume percent retained austenite was determined using the direct comparison method of Averbach and Cohen<sup>16</sup> in accordance with ASTM E975 and SAE SP-453.

### **High Cycle Fatigue Testing**

High cycle fatigue tests were performed in 4 point bending under constant amplitude loading. A photograph of the fatigue test setup is shown in Figure 1.

Fatigue testing was conducted at ambient temperature ( $\sim 25^\circ\text{C}$ ) and frequency of 30 Hz at an R-ratio of 0.1. Notches of 0.010 in. (0.25 mm) were used to simulate contact (pitting fatigue) damage. Notching was performed using electrical discharge machining (EDM) Figure 2 shows the location of the EDM notch on the specimen. Specimens were tested in Baseline (Ground), SP, and LPB conditions. For each condition, one set of specimens was tested without a notch (smooth) and one set was tested with a notch. Following fatigue testing, each specimen was examined optically to identify the location of the fatigue failure initiation.



Figure 1: HCF Test Set Up for Testing a Thick Section Specimen.

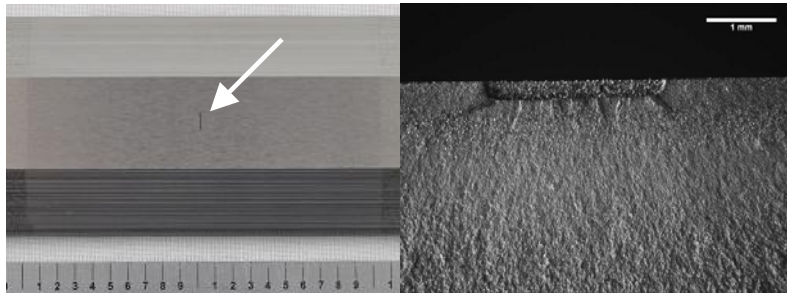


Figure 2: Photographs Showing the Location of the 0.1 in. Long x 0.010 in. Deep EDM Notch on the Top Face of the Specimen. The Notch is Shown on an Untested Specimen on the Left and on the Fracture Face of a Tested Specimen on the Right.

### Stability of Residual Stress

The effect of cyclic loading on the stability of residual stresses in LPB treated specimens was investigated. This was accomplished by comparing residual stress distributions in LPB treated specimens both before and after HCF testing was performed.

The effect of mechanical overload on the stability of residual stresses was investigated. To accomplish this two specimens were prepared by low stress grinding (LSG). One specimen was shot peened on both surfaces and the second specimen was LPB processed on both surfaces. The specimens were deformed in 3-point bending to a predetermined maximum plastic strain level at mid-point, creating a plastic strain gradient as a function of distance from the mid-point. Therefore, a single specimen could be used to test the effect of tensile (bottom surface) and compressive (top surface) overload. Surface residual stresses were measured by x-ray diffraction (XRD) methods as a function of distance along the length of the specimens. Each sample was displaced a total of 0.8 in. (20.3 mm) at mid-length (center) in the bending fixture. The maximum plastic deformation at the sample center was approximately 1.3% for the shot peen sample and approximately 1.4% for the LPB processed sample. The plastic deformation was of low magnitude for both samples beyond 3 in. (76.2 mm) from the center. XRD residual stress measurements were made at the surface, in the longitudinal direction, on both the compressive and tensile applied stress sides. Measurements were made from the center of the bend out to a distance where the plasticity from bending was at or near zero.

The effect of thermal relaxation on the stability of residual stresses was also investigated. To accomplish this two specimens were prepared by low stress grinding (LSG). One specimen was SP on both surfaces and the remaining specimen was LPB treated on both surfaces. The effect

of thermal exposure was studied by exposing each specimen to temperatures ranging from 156°C to 192°C (312.8 – 377.6°F) for 24 hours in a linear tube furnace. Surface residual stresses were measured by x-ray diffraction methods as a function of position / temperature along the length of the specimens after thermal exposure.

### Surface Roughness

The surface roughness of the LPB treated thick section specimens after processing was compared to the Baseline (ground) and SP treated HCF specimens. Surface roughness value, Ra, was an averaged of 3 passes over 0.150 in. (3.8 mm) transverse to the specimen axis, and over 0.5 in. (12.7 mm) longitudinal with the specimen.

## RESULTS

### Residual Stresses

Figure 3 contains a plot of the residual stress distribution for the baseline (ground), SP, and LPB processed conditions. The baseline condition shows a compressive layer at a nominal stress level of approximately –75 ksi. In the SP condition, the surface compression of –140 ksi changes as a function of depth and a maximum compression of –220 ksi is seen at a depth of approximately 0.002 in. (0.05 mm). The stress then gradually decreases to approximately –50 ksi at depths of 0.010 in. (0.25 mm) and beyond. LPB processed specimens shows a surface compression of –140 ksi, which gradually increases to approximately –270 ksi at a depth of 0.005 in. (0.13 mm), and further gradually decreases to near zero at a depth of 0.030 in. (.76 mm). The higher magnitude and depth of compression provided by LPB processing when compared to SP provides greater fatigue strength and helps mitigate the effect of contact fretting damage fatigue performance. The benefit on fatigue performance that LPB processing provides is discussed in detail in the experimental results section for HCF testing.

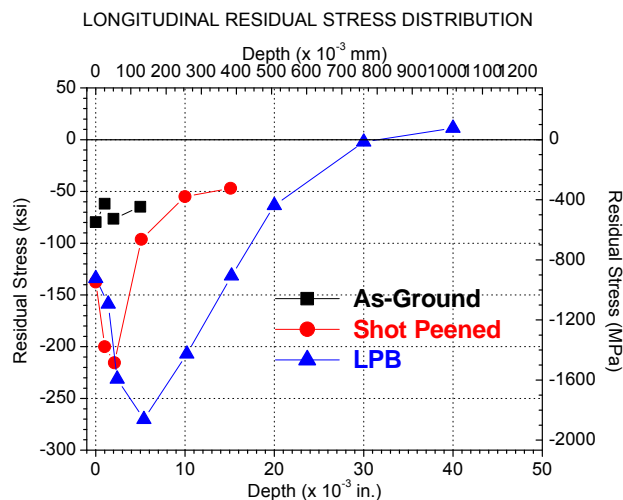


Figure 3: Plot of Residual Stress vs. Depth in the As-Ground, Shot Peened and LPB Treated Carburized and Heat Treated 9310 Gear Steel Specimens.

## Retained Austenite

The mean volume percent retained austenite is presented in Figure 4. The surface austenite content is approximately 17%, which remains the same as a function of depth for the baseline specimen. For the SP specimen the retained austenite reduces to approximately 9% at a depth of 0.001 in. (0.03 mm) and then gradually increases to approximately 15% at depths beyond 0.005 in. (0.13 mm). In the LPB treated specimen the retained austenite decreases to approximately 8% to a depth of 0.005 in. (0.13 mm) and then gradually increases to approximately 12% at depths beyond 0.020 in. (0.51 mm). The implications on fatigue performance due to a change in volume percent austenite were not studied in this investigation.

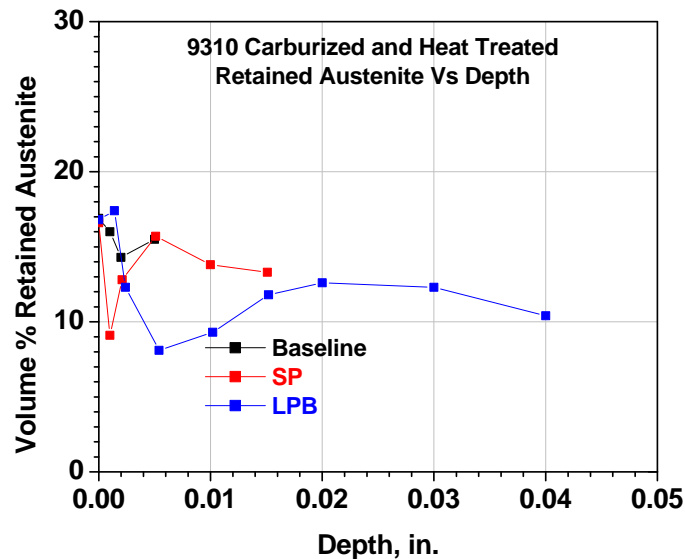


Figure 4: Plot of % Retained Austenite vs Depth for Baseline, Shot Peened and LPB Treated Specimens.

## High Cycle Fatigue

Fatigue testing results are presented graphically in Figure 5 as S-N plots. The data are shown in a semi-log plot of maximum stress in units of ksi ( $10^3$  psi) and MPa vs. cycles to failure. The arrows indicate a run-out condition ( $10^7$  cycles).

The baseline (ground) specimens demonstrated a nominal fatigue strength ( $S_{max}$  for  $R = 0.1$  and  $10^7$  cycles) of 200 ksi, this dropped to approximately 60 ksi with the introduction of the EDM notch, indicating a fatigue debit of  $> 3$ . The SP specimens showed a slightly better fatigue strength of approximately 220 ksi in the smooth condition and approximately 100 ksi with an EDM notch, indicating a fatigue debit of approximately 2. The LPB treated specimens demonstrated a fatigue strength of approximately 240 ksi in the smooth condition and approximately 170 ksi with the notch, indicating a fatigue debit of approximately 1.4.

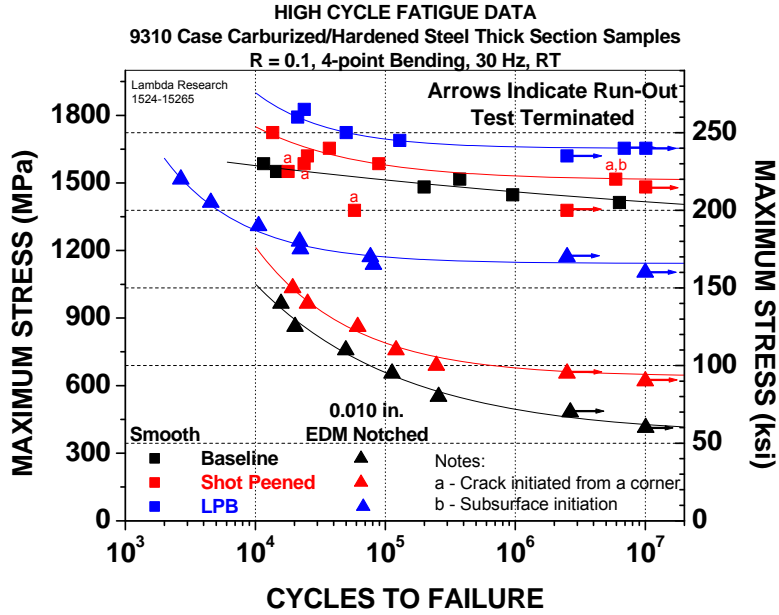


Figure 5: Fatigue Test Results

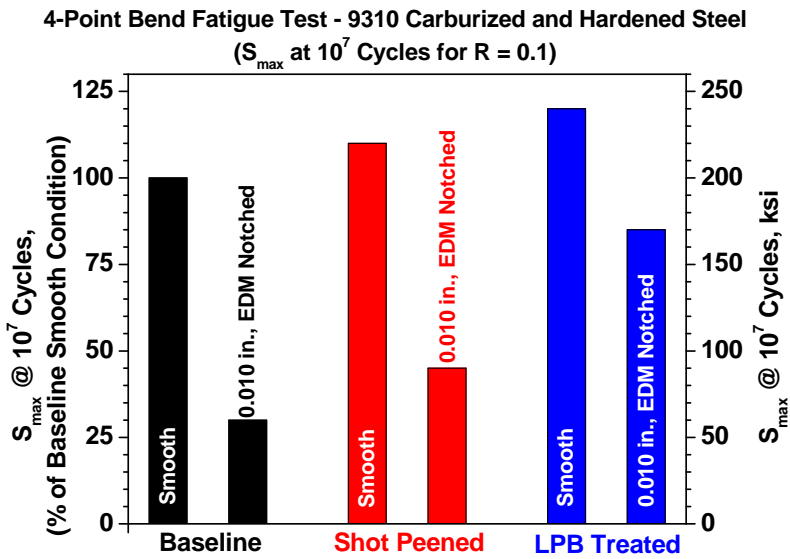


Figure 6: HCF Performance of Untreated, Shot Peened, and LPB Treated Posts With and Without a 0.010 in. Deep EDM Notch to Simulate Contact (Pitting) Damage on the Gear Tooth.

HCF test results are also presented graphically in the form of a bar chart in Figure 6. The fatigue strength of the baseline smooth parts is defined to be 100%. As shown here, the baseline specimens with the EDM notch condition have a fatigue strength loss of over 70% of that of the baseline smooth condition. Similarly, while the SP smooth condition shows a 10% improvement over the baseline smooth, the introduction of an EDM notch still leads to over 50% reduction in fatigue strength. LPB treated smooth specimens showed a 20% improvement over the baseline smooth condition and a 10% improvement over the shot peened smooth condition. With the introduction of an EDM notch the fatigue strength dropped only by approximately 15% compared to the baseline smooth condition.

The increase in fatigue performance that LPB processing provides can lower maintenance cost for drive train components. This would be achieved by lengthening the time interval between inspections. LPB processing can provide a higher allowable load on gear teeth for a given dimensional or weight requirement.

Following fatigue testing, each specimen was examined optically to identify the location of the fatigue origins. Shown below in Figure 7 are typical fracture surfaces of baseline (9a), SP (9b), LPB processed (9c), and notched specimens (9d). All notched specimen's failures initiated from the notch so only one process condition is shown, LPB processed.

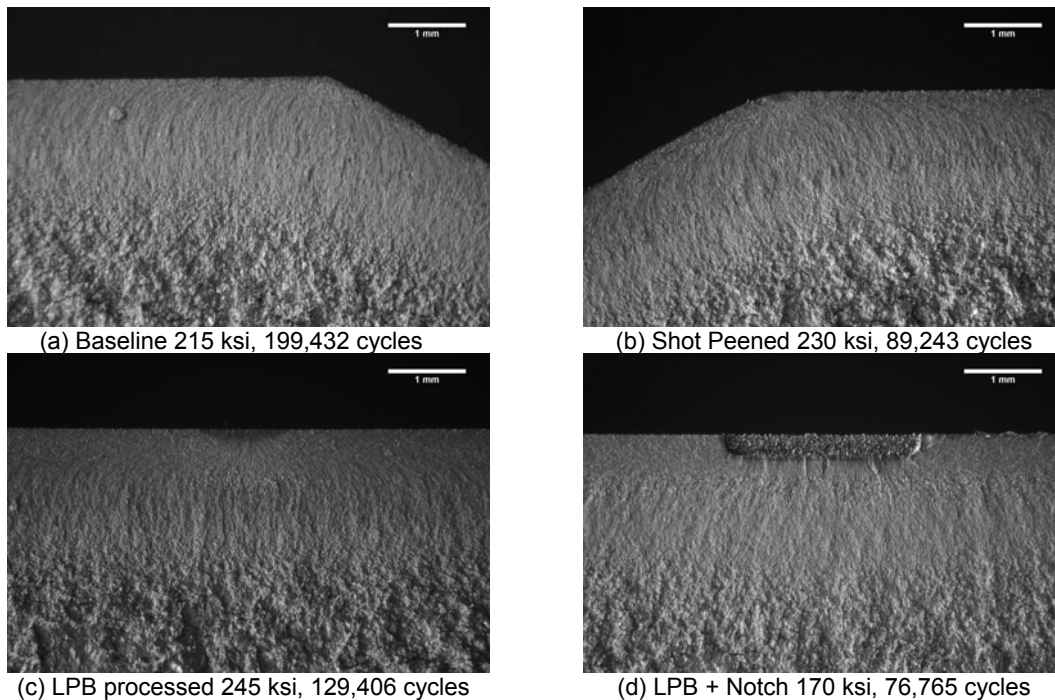


Figure 7: Typical fracture faces from HCF test specimens

## Stability of Residual Stress

### Mechanical Cyclic Relaxation

Figure 8 shows the residual stress distributions in an LPB treated and surface ground specimen in both the untested and fatigue tested condition. As seen here, there is little or no relaxation of residual stresses after mechanical cyclic loading at an  $S_{max}$  of 245 ksi. This shows that during operation the residual compressive stress induced by the LPB process will not relax due to elastic cyclic loading.

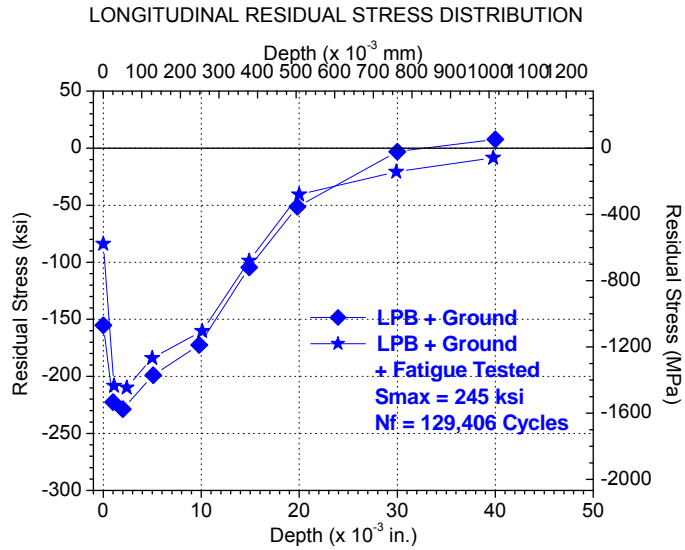


Figure 8: Residual Stresses in LPB Treated Specimens Before and After Fatigue Testing.

### Mechanical Overload Relaxation

A comparison of surface residual stresses between the LPB treated and SP samples are shown in Figure 9a. A corresponding residual stress distribution at a depth of 0.005 in. (0.13 mm) for both LPB treated and SP samples are shown in Figure 9b. Results are shown on a semi-logarithmic plot in these figures to expand the scale at the relatively low plastic strain levels.

As shown in Figure 9a, on the surface, both LPB and SP resulted in similar residual stress distributions. Similar variations in residual stresses after plastic deformation were observed for the two surface treatments on both the tensile and compressive sides. For both treatments, the residual stresses were not seen to relax for plastic deformation up to approximately 0.4% and some relaxation of residual stresses were observed for plastic strain above 0.4%. The tensile overload appears to result in greater relaxation of residual stresses compared to the compressive overload.

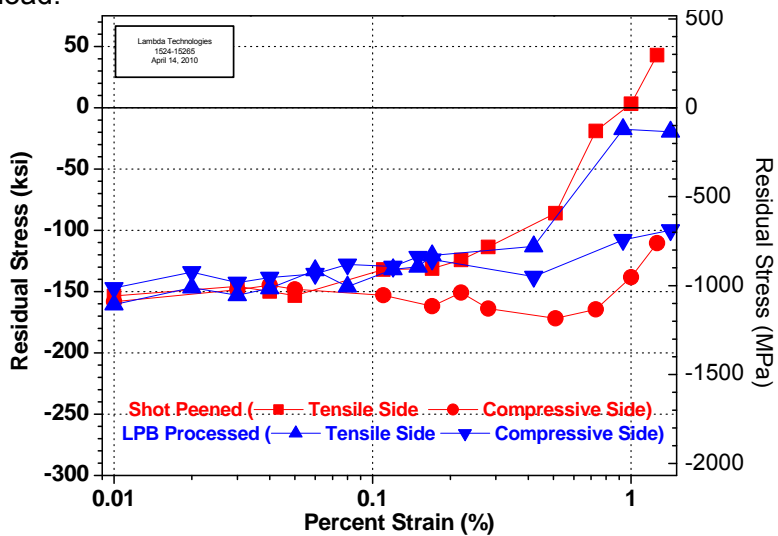


Figure 9a: Comparison of Surface Residual Stress as a Function of Bulk Plastic Deformation in Carburized and Heat Treated 9310 Gear Steel 3-Point Bend Beams.

At a depth of 0.005 in. (0.13 mm), the LPB processed specimen showed a higher magnitude of compression, (-250 to -280 ksi), while the SP specimen showed a lower magnitude of compression (-110 to -150 ksi). Although both specimens showed relaxation of residual stresses at plastic deformation greater than 0.4%, due to the initial high magnitude of compression for the LPB processed specimen, it retained a substantial amount of compressive residual stresses, even at plastic strain levels greater than 1%. In contrast, the SP specimen showed nearly complete stress relaxation and even transition of the residual stresses from compression to tension at high plastic strain.

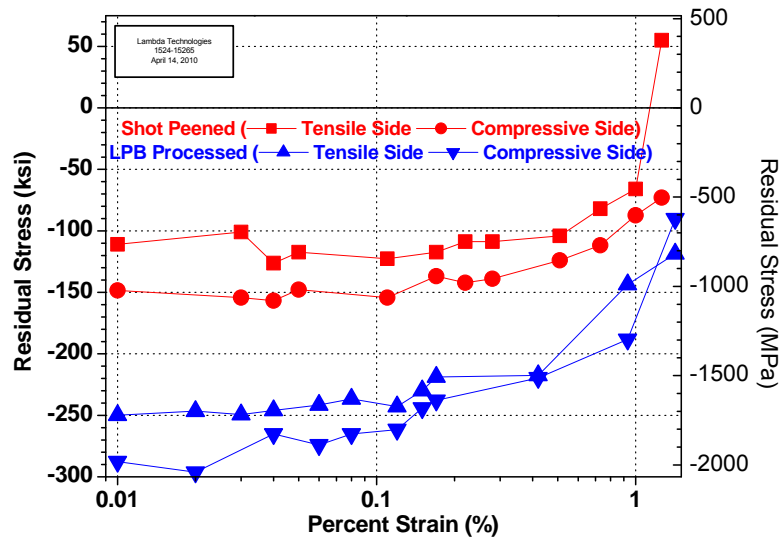


Figure 9b: Comparison of Residual Stress as a Function of Bulk Plastic Deformation at a Depth of 0.005 in. in Carburized and Heat Treated 9310 Gear Steel 3-Point Bend Beams.

### Thermal Relaxation

The results shown in Figure 10 show the effect of thermal exposure on the relaxation of surface residual stresses from SP and LPB processing. Residual stress measurements were made on the thermally exposed surfaces and at a depth of 0.005 in. (0.13 mm) in both SP and LPB treated specimens.

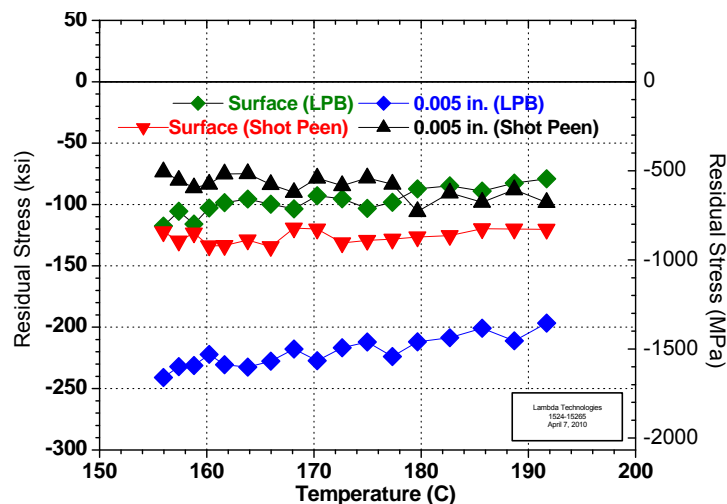


Figure 10: Comparison of Shot Peened and LPB'ed Residual Stress for 9310 Steel Carburized Steel Exposed at Temperatures of 156C to 192C C for 24 Hrs.

As seen in this figure, very little relaxation of residual stresses result from thermal exposure for both the shot peened and the LPB treated specimens. As observed before, the near surface compression for both surface treatments are similar, while at the 0.005 in. (0.13 mm) depth, the LPB treated specimens show higher magnitude of compression. This is a result of the depth of compression introduced by LPB.

## Surface Roughness

The results of the surface roughness measurements for each process are shown in Figure 11 in the form of a bar chart. The surface roughness is lowest for the LPB process, indicating a smoother surface as compared to the ground or shot peened surfaces. Smoother surfaces lead to less friction between gear teeth and ultimately greater contact fatigue life. Lower friction also reduces noise and oil / material temperature.

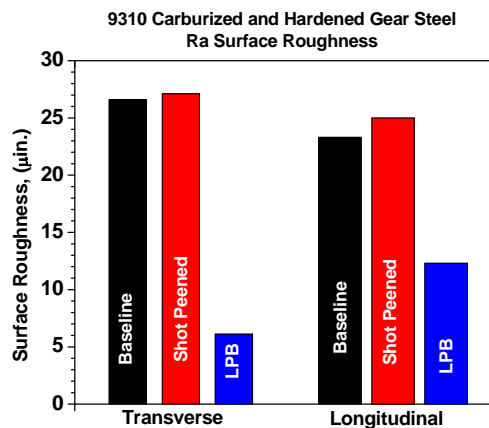


Figure 11: Bar Chart Showing the Comparison of the Surface Roughness of Baseline (Ground) and Shot Peened Specimens versus LPB Treated Specimens.

## CONCLUSIONS

A comprehensive study was undertaken to demonstrate the benefits of using LPB technology to introduce controlled distribution of compressive residual stresses to improve fatigue performance and damage tolerance in carburized and heat treated 9310 gear steels used in rotorcraft gears. The following conclusions may be reached from this study:

- LPB processing produces compressive residual stresses for depths up to 3X greater than SP. The peak compressive residual stress for LPB is 20% greater than for SP.
- In smooth condition, LPB leads to a 10% improvement in fatigue strength over SP.
- With the presence of a 0.010 in. (0.25 mm) deep EDM notch, LPB leads to nearly a 100% improvement in fatigue strength over SP.
- The compressive residual stresses from LPB are stable and did not show significant relaxation after cyclic loading.
- Both LPB and SP treatments show similar surface residual stress relaxation after a single cycle of mechanical overload. However, at a depth of 0.005 in. (0.13 mm) SP leads to either a complete relaxation or even flipping into tension after the overload cycle, while the compressive residual stresses are maintained for LPB.
- There is very little relaxation of the residual stresses observed for either treatment due to thermal exposure for 24 hours in the temperature range of 150-200°C.

- LPB produces a much smoother surface, with a surface roughness of 5 – 10  $\mu\text{in}$ , while the SP leads to a relatively rough surface with 25  $\mu\text{in}$  of Ra surface roughness.

In summary, the LPB treatment has been demonstrated to have improved the fatigue performance over the standard shot peening treatment in carburized and heat treated 9310 gear steels, and improve the resistance to simulated contact pitting damage. This demonstration paves the way for developing applications of this technology for actual gears by appropriate design of LPB tools and implementation of the designed residual stresses to improve the performance of rotorcraft gears.

## Acknowledgment

Funding from the Army SBIR program Topic No. A09-014, Contract No. W911W6-10-C-0005 (TPOC: Clay Ames, AATD) is gratefully acknowledged. The authors also wish to thank Steve Hammond for the assistance provided by Rolls Royce, Indianapolis with the carburizing and heat treatment of specimens, and for technical discussions.

---

## Reference:

- 1 John S. Eckerseley, Editor, "Review of Shot Peening Technology – Gearing Up for Higher Loads", Metal Improvement Company, Document # 93099, Spring 1993
- 2 Katsumi Inoue, Masana Kato, "Estimation of Fatigue Strength Enhancement for Carburized and Shot-Peened Gears", Journal of Propulsion and Power, Vol. 10, No.3, May-June 1994, pp 362-368
- 3 Dennis P. Townsend, "Improvements in Surface Fatigue Life of Hardened Gears by High Intensity Shot Peening", NASA Technical Memorandum 105678, DTIC Publication dated June 17, 1992
- 4 Dale W. Schwach, Y.B. Gao, "A Fundamental Study on the Impact of Surface Integrity by Hard Turning on Rolling Contact Fatigue", Transaction of NAMRI/SME Vol. 33, 2005 pp 541-548
- 5 Lane Winkelmann, "Gear Isotropic Finish Generation General Process Control and Alternate Tooth by Tooth Process For Large Gears, 2006 CTMA Symposium, Williamsburg, VA March 27-29, 2006
- 6 Robert P. Garibay, Nam S. Chang, "Improved Fatigue Life of a Carburized Gear By Shot Peening Parameter Optimization"
- 7 Prev y, P.S., Cammett J.T., "The Effect of Shot Peening Coverage on Residual Stress, Cold Work and Fatigue in a Ni-Cr-Mo Low Alloy Steel" Proc. International Conference on Shot Peening, 2002.
- 8 Hanagarth, H., V hringer, O., and Macherauch, E., Shot Peening, Jap. Soc. of Prec. Engrg., Tokyo, Japan, 337-345 (1993)
- 9 V hringer, O., Residual Stresses, DGM Informationsgesellschaft-Verlag, Oberursel, 47-80 (1986)
- 10 Hilley, M.E. ed., (1971), Residual Stress Measurement by X-Ray Diffraction, *SAE J784a*, Warrendale, PA: Society of Auto. Eng.)
- 11 Noyan, I.C. and Cohen, J.B., (1987) Residual Stress Measurement by Diffraction and Interpretation, (New York, NY: Springer-Verlag).
- 12 Cullity, B.D., (1978) Elements of X-ray Diffraction, 2nd ed., (Reading, MA: Addison-Wesley), pp.447-476.
- 13 Prev y, P.S., (1986), "X-Ray Diffraction Residual Stress Techniques," *Metals Handbook*, **10**, (Metals Park, OH: ASM), pp 380-392.
- 14 Koistinen, D.P. and Marburger, R.E., (1964), Transactions of the ASM, **67**.
- 15 Moore, M.G. and Evans, W.P., (1958) "Mathematical Correction for Stress in Removed Layers in X-Ray Diffraction Residual Stress Analysis," SAE Transactions, **66**, pp. 340-345.
- 16 B.L. Averbach and M. Cohen, Trans. AIME, Vol. 176, 1948, p. 401.